

Modification of nuclear mass formula by considering isospin effectsNing Wang,^{1,*} Min Liu,^{1,2} and Xizhen Wu³¹*Department of Physics, Guangxi Normal University, Guilin 541004, People's Republic of China*²*College of Nuclear Science and Technology, Beijing Normal University, Beijing, 100875, People's Republic of China*³*China Institute of Atomic Energy, Beijing 102413, People's Republic of China*

(Received 2 December 2009; revised manuscript received 12 April 2010; published 30 April 2010; corrected 4 May 2010)

We propose a semiempirical nuclear mass formula based on the macroscopic-microscopic method in which the isospin and mass dependence of model parameters are investigated with the Skyrme energy density functional. The number of model parameters is considerably reduced compared with the finite range droplet model. The rms deviation with respect to 2149 measured nuclear masses is reduced by 21%, falling to 0.516 MeV. The new magic number $N = 16$ in light neutron-rich nuclei and the shape coexistence phenomena for some nuclei have been examined with the model. The shell corrections of superheavy nuclei are also predicted.

DOI: [10.1103/PhysRevC.81.044322](https://doi.org/10.1103/PhysRevC.81.044322)

PACS number(s): 21.10.Dr, 21.30.Fe

I. INTRODUCTION

The nuclear mass is of great importance not only for various aspects of nuclear physics but also for weak-interaction studies and astrophysics [1]. In nuclear physics, it is helpful to study the nuclear symmetry energy and the synthesis of superheavy nuclei by considering the more than 2000 measured nuclear masses. Theoretically, the mass of an atomic nucleus can be calculated by the macroscopic-microscopic method (such as the finite-range droplet model [2]) or the microscopic approaches (such as the Hartree-Fock Bogoliubov approach [3,4]) or some other mass formulas [5]. The best mass formulas at present can reach about 0.6 MeV in the rms deviation for the usual data set of 2149 measured masses of nuclei (N and $Z \geq 8$) [6] with about 24 \sim 30 model parameters. Compared with the microscopic Hartree-Fock (HF) approaches, the macro-micro model is much faster in the calculation of the nuclear masses for the whole nuclear chart which provides a possibility for performing large-scale nuclear mass calculations to refine the model parameters and to explore the global behavior of nuclei. However, there are two crucial points in the macro-micro method that should be further studied. The first is that the consistency of the model parameters between the macroscopic and microscopic parts in the macro-micro method should be improved. It is known that although the finite-range droplet model (FRDM) is widely used in the calculations of nuclear mass, the parameter values in the calculation of the microscopic shell corrections differ from the corresponding values used in the macroscopic part of the model [1]. This less consistency between the macroscopic and microscopic parts may considerably reduce the credibility of extrapolations of the macroscopic-microscopic approach. On the other hand, with the great development of the experimental facilities for the study on superheavy nuclei and nuclei far from the β -stability line, the influence of isospin effects on the nuclear mass formula attracted great attention and should be given better consideration. Based on the above discussions, an improved nuclear mass formula that

self-consistently considers the isospin effects in both macroscopic and microscopic parts would need to be established to provide large-scale nuclear mass calculations.

To investigate the consistency of the model parameters between the macroscopic and microscopic parts in the macroscopic-microscopic approach and isospin dependence of the model parameters, the Skyrme energy density functional approach together with the extended Thomas-Fermi (ETF) approximation [7,8] is used. It is known that the energy-density functional theory is widely used in the study of the nuclear ground state which provides us with a useful balance between accuracy and computation cost allowing large systems with a simple self-consistent manner. With the Skyrme energy density functional approach, we systematically investigate some ground state properties of nuclei, such as the nuclear symmetry energy coefficient, the deformation energy, and the symmetry potential, which are helpful to improve the macro-micro method. Based on these calculations, we propose a semiempirical nuclear mass formula by taking into account the isospin- and mass-dependent model parameters. The article is organized as follows. In Sec. II, the proposed mass formula is introduced. In Sec. III, some calculation results are presented. Finally, a summary is given in Sec. IV.

II. THE MODEL

In this section, we first introduce the macroscopic part of the mass formula. Then, the influence of nuclear deformation on the macroscopic energy of nucleus is investigated with the Skyrme energy-density functional approach, and the single-particle potential used in the calculation of the microscopic shell correction is introduced. In addition, the symmetry potential and the symmetry energy coefficient of nuclear matter is also investigated. Finally, the parameters adopted in the model are presented.

A. Modified Bethe-Weizsäcker mass formula

We start with the macroscopic-microscopic method [2,9]. The total energy of a nucleus can be calculated as a sum of the

* wangning@gxnu.edu.cn

liquid-drop energy and the Strutinsky shell correction ΔE ,

$$E(A, Z, \beta) = E_{\text{LD}}(A, Z) \prod_{k \geq 2} (1 + b_k \beta_k^2) + \Delta E(A, Z, \beta). \quad (1)$$

The liquid-drop energy of a spherical nucleus $E_{\text{LD}}(A, Z)$ is described by a modified Bethe-Weizsäcker mass formula [10],

$$E_{\text{LD}}(A, Z) = a_v A + a_s A^{2/3} + a_c \frac{Z(Z-1)}{A^{1/3}} (1 - Z^{-2/3}) + a_{\text{sym}} I^2 A + a_{\text{pair}} A^{-1/3} \delta_{np} \quad (2)$$

with isospin asymmetry $I = (N - Z)/A$. The pairing term proposed in Ref. [11] is adopted, with

$$\delta_{np} = \begin{cases} 2 - |I| : N \text{ and } Z \text{ even} \\ |I| : N \text{ and } Z \text{ odd} \\ 1 - |I| : N \text{ even, } Z \text{ odd, and } N > Z \\ 1 - |I| : N \text{ odd, } Z \text{ even, and } N < Z \\ 1 : N \text{ even, } Z \text{ odd, and } N < Z \\ 1 : N \text{ odd, } Z \text{ even, and } N > Z. \end{cases} \quad (3)$$

In this work, the symmetry energy coefficient of finite nuclei is written as,

$$a_{\text{sym}} = c_{\text{sym}} \left[1 - \frac{\kappa}{A^{1/3}} + \frac{2 - |I|}{2 + |I|A} \right], \quad (4)$$

based on the conventional surface-symmetry term [12,13] of liquid-drop model, with a small correction term for description of isospin dependence of a_{sym} . The sensitive dependence of the symmetry energy coefficient on the asymmetry of the nucleus, especially that a_{sym} increases with increasing proton fraction of the system, is also found in Ref. [14]. The introduced I correction term approximately describes the Wigner effect [2] of heavy nuclei. For a heavy nucleus near the β -stability line ($A|I| \gg 2 \gg |I|$), the introduced I term in a_{sym} roughly leads to a correction $c_{\text{sym}} \frac{(2-|I|)I^2 A}{2+|I|A} \approx 2c_{\text{sym}}|I|$ (known as Wigner term) to the binding energy of the nucleus. Compared with the case without the I term being taken into account, the rms deviation of nuclear masses defined as $\sigma^2 = \frac{1}{m} \sum (M_{\text{exp}}^{(i)} -$

$M_{\text{th}}^{(i)})^2$ from the measured masses AME2003 [6] for the 2149 nuclei (N and $Z \geq 8$) is reduced by about 6%. Furthermore, we find when the isospin dependence of the symmetry energy coefficient is taken into account, the obtained optimal c_{sym} increases about 3 MeV and up to 29 MeV, which is close to the symmetry energy coefficient of nuclear matter at saturation density obtained from the Skyrme energy-density functional.

The Coulomb exchange correction and surface diffuseness correction to the Coulomb energy is approximately taken into account as the term $Z^{-2/3}$. In addition, the terms b_k in Eq. (1) which are obtained according to the Skyrme energy-density functional (the detailed discussion is in the next subsection) describe the contribution of nuclear deformation to the macroscopic energy.

B. Influence of nuclear deformation on the macroscopic energy

For the deformation of nuclei, we consider only axially deformed cases. In this work, only β_2 and β_4 deformations of nuclei are taken into account. We first investigated the energy of a nucleus with respect to a β_2 deformation based on the Skyrme energy-density functional together with the extended Thomas-Fermi approximation (ETF) [7,8]. The procedure is as follows: The total energy of a nucleus can be expressed as the integral over the Skyrme energy-density functional $\mathcal{H}(\mathbf{r})$ [15]. Given a density functional $\rho(\mathbf{r})$, one can calculate the corresponding energy via $E = \int \mathcal{H}[\rho(\mathbf{r})] d\mathbf{r}$ under the ETF approximation. We first obtain the binding energy E_0 and the spherical Woods-Saxon density distributions of a nucleus with the approach in Ref. [8]. Then, with the same procedure, we calculate the energy $E(\beta_2)$ of the nucleus with a quadrupole deformed Woods-Saxon density distribution of the nucleus in which the central density and the surface diffuseness remained unchanged. Figure 1(a) shows the calculated energy of ^{16}O , ^{48}Ca , and ^{208}Pb as a function of β_2 deformation with the SkM* interaction [15] (denoted by circles). The solid curves denote the results of a formula $E/E_0 = 1 + b_2 \beta_2^2$ in which the value of b_2 is obtained by fitting the open circles. One can see that the parabola approximation to the change of energy with β_2 is acceptable. Figure 1(b) shows the value of b_2 as a function of

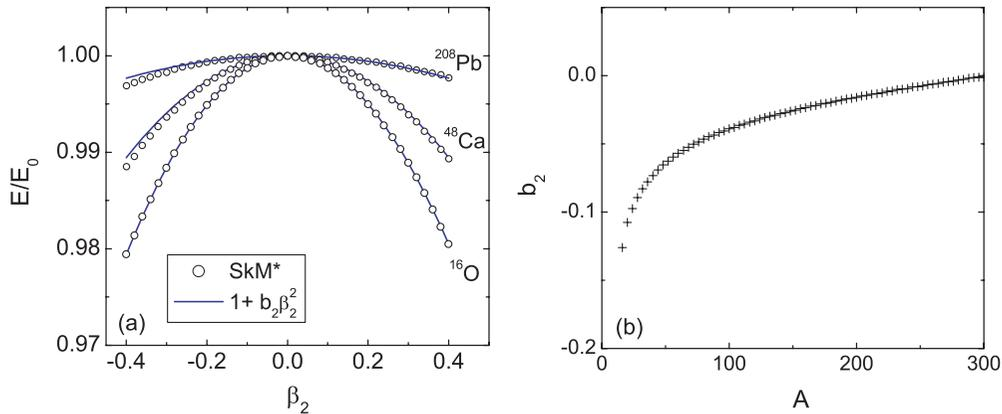


FIG. 1. (Color online) (a) Energy of ^{16}O , ^{48}Ca , and ^{208}Pb with respect to β_2 deformation. Here, the values of E_0 are negative. The circles and the solid curves denote the results of SkM* interaction and of a formula $E/E_0 = 1 + b_2 \beta_2^2$, respectively. (b) The value of b_2 obtained with SkM* as a function of mass number.

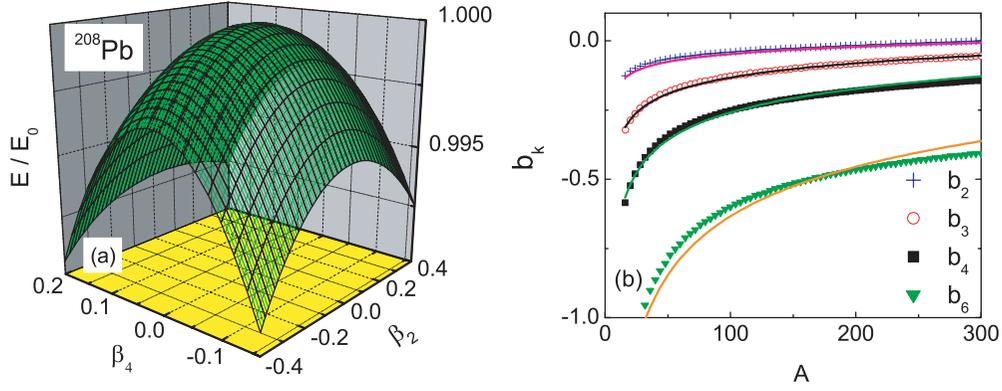


FIG. 2. (Color online) (a) Energy of ^{208}Pb with respect to β_2 and β_4 deformation with Skyrme energy-density functional approach. (b) The value of b_k as a function of mass number. The scattered symbols denote the obtained curvatures of the parabolas with the Skyrme force SkM* for a number of nuclei. The solid curves denote the corresponding results with an empirical formula (6).

the mass number. The crosses denote the results of the SkM* interaction for a number of nuclei along the β -stability line. We find that the dependence of b_2 on the mass number A can be reasonably well described by the formula

$$b_2 = g_1 A^{1/3} + g_2 A^{-1/3}. \quad (5)$$

This form of mass dependence of b_2 is therefore adopted in the proposed mass formula and the optimal values of g_1 and g_2 are finally determined by the 2149 measured nuclear masses [6].

To take into account the influence of the higher-multipole deformation of nuclei, we investigate the change of energy of a nucleus with respect to a certain set of nuclear deformation parameters with the Skyrme energy-density functional approach mentioned previously. In Fig. 2(a), we show the energy of ^{208}Pb as a function of β_2 and β_4 with the Skyrme force SkM*. We find that the influence of nuclear β_4 deformation on the nuclear energy can be roughly described by a parabola at small deformations. For other higher-multipole deformations, the parabola approximation can also be applied for small deformation cases, and the proposed model can be easily extended to consider other higher-multipole deformations. Furthermore, we notice that the curvature of the parabola for a given β_k deformation can be approximately described by an empirical formula

$$b_k = \left(\frac{k}{2}\right) g_1 A^{1/3} + \left(\frac{k}{2}\right)^2 g_2 A^{-1/3}, \quad (6)$$

which is an extension of the formula (5). In Fig. 2(b), we show the mass-dependent curvatures of the parabolas. The crosses, the open circles, the solid squares, and the triangles denote the obtained curvatures b_2 , b_3 , b_4 , and b_6 of the parabolas with the Skyrme energy-density functional approach for a number of nuclei along the β -stability line, respectively. The solid curves denote the corresponding results with the empirical formula (6) taking $g_1 = 0.0074$ and $g_2 = -0.38$. One can see that the curvatures of the parabolas can be reasonably well described by the empirical formula which greatly reduces the computation time for the calculation of deformed nuclei.

C. Single-particle potential in the microscopic part

In the microscopic part, the shell correction

$$\Delta E = c_1 E_{\text{sh}} \quad (7)$$

is obtained by the traditional Strutinsky procedure [16] by setting the smoothing parameter $\gamma = 1.2\hbar\omega_0$ and the order $p = 6$ of the Gauss-Hermite polynomials, where $E_{\text{sh}} = E_{\text{sh}}(P) + E_{\text{sh}}(N)$, i.e., the sum of the shell energies of protons and neutrons and $\hbar\omega_0 = 41A^{-1/3}$ MeV is the mean distance between the gross shells. In this work, we introduce a scale factor c_1 to the shell correction. This additional parameter is used to adjust the division of the binding energy between the macroscopic part and the remaining microscopic correction. It is known that a similar scale factor is usually introduced to the liquid-drop part [17] or the shell-correction part [18] to adjust the division between the two parts for giving better results in the calculation of fission barrier. It is necessary to investigate the influence of this parameter on the nuclear masses. We find that the rms deviation for the 2149 nuclear masses can be somewhat reduced with the introduced factor c_1 compared with the case setting $c_1 = 1$.

To obtain the shell-correction ΔE , we execute a computer code WSBETA [19] to calculate the single-particle levels of an axially deformed Woods-Saxon potential and then perform the Strutinsky procedure. The single-particle Hamiltonian in the code WSBETA is written as

$$H = T + V + V_{\text{s.o.}}, \quad (8)$$

with the spin-orbit potential

$$V_{\text{s.o.}} = -\lambda \left(\frac{\hbar}{2Mc}\right)^2 \nabla V \cdot (\vec{\sigma} \times \vec{p}), \quad (9)$$

where λ denotes the strength of the spin-orbit potential. In this work, we set $\lambda = \lambda_0(1 + \frac{N_i}{A})$ with $N_i = Z$ for protons and $N_i = N$ for neutrons. Here, the isospin-dependent spin-orbit interaction strength is obtained based on the Skyrme energy-density functional in which the spin-orbit potential is usually

expressed as

$$\begin{aligned} V_q^{\text{s.o.}} &= \frac{1}{2} W_0 \nabla(\rho + \rho_q) \cdot (\vec{\sigma} \times \vec{p}) \\ &\approx \frac{1}{2} W_0 \left(1 + \frac{N_i}{A} \right) \nabla \rho \cdot (\vec{\sigma} \times \vec{p}), \end{aligned} \quad (10)$$

with the nucleon density $\rho = \rho_p + \rho_n$ and the spin-orbit strength W_0 . In Eq. (9) M is the free nucleonic mass and $\vec{\sigma}$ and \vec{p} are the Pauli spin matrix and the nucleon momentum, respectively [19]. The central potential V is described by an axially deformed Woods-Saxon form

$$V(\vec{r}) = \frac{V_q}{1 + \exp\left[\frac{r - \mathcal{R}(\theta)}{a}\right]}, \quad (11)$$

where the depth V_q of the central potential ($q = p$ for protons and $q = n$ for neutrons) is written as

$$V_q = V_0 \pm V_s I \quad (12)$$

with the plus sign for neutrons and the minus sign for protons. V_s is the isospin-asymmetric part of the potential depth. We assume $V_s = a_{\text{sym}}$ in this work (detailed study of the relation between V_s and a_{sym} is given in the following part of this section). \mathcal{R} defines the distance from the origin of the coordinate system to the point on the nuclear surface

$$\mathcal{R}(\theta) = c_0 R [1 + \beta_2 Y_{20}(\theta) + \beta_4 Y_{40}(\theta) + \dots], \quad (13)$$

with the scale factor c_0 which represents the effect of incompressibility of nuclear matter in the nucleus and is determined by the so-called constant volume condition [19]. $Y_{lm}(\theta, \phi)$ are the spherical harmonics. $R = r_0 A^{1/3}$ and a denote the radius and surface diffuseness of the single-particle potential, respectively. Here, we assume and set the radius and diffuseness of the single-particle potential of protons equal to those of neutrons for simplicity. For protons the Coulomb potential is additionally involved (see Ref. [19] for details).

D. Symmetry potential and symmetry energy coefficient

The relation between the isospin-asymmetric part V_s of the single-particle potential depth in the microscopic part and the symmetry energy coefficient in the macroscopic part is investigated based on the Skyrme energy-density functional together with the ETF approach. In this approach, the central one-body potential is described by $V_q = \frac{\delta \varepsilon(\mathbf{r})}{\delta \rho_q(\mathbf{r})}$ with the energy-density functional $\varepsilon(\mathbf{r})$ (see Eq. (9) in Ref. [7] for details). The difference between the neutron ($q = n$) and proton ($q = p$) potentials of nuclear matter is written as

$$\begin{aligned} V_n - V_p &= 2B_2 \rho \delta + 2B_8 \rho^{\alpha+1} \delta + B_4 (\tau_n - \tau_p) \\ &= 2B_2 \rho \delta + 2B_8 \rho^{\alpha+1} \delta + B_4 c_k \rho^{5/3} \delta + \mathcal{O}(\delta^3) \end{aligned} \quad (14)$$

with the kinetic energy density τ_q which can be expressed as $\tau_q = \frac{3}{5} (3\pi^2)^{2/3} \rho_q^{5/3}$ in the Thomas-Fermi approximation, the isospin asymmetry $\delta = (\rho_n - \rho_p)/\rho$, and the coefficient $c_k = (3\pi^2/2)^{2/3}$. B_2 , B_8 , and B_4 (notations in Ref. [7]) are some combinations of Skyrme parameters, given by $B_2 = -\frac{1}{2} t_0 (\frac{1}{2} + x_0)$, $B_8 = -\frac{1}{12} t_3 (\frac{1}{2} + x_3)$, and $B_4 = -\frac{1}{4} [t_1 (\frac{1}{2} + x_1) - t_2 (\frac{1}{2} +$

$x_2)]$. The symmetry potential V_{sym} may be written as

$$V_{\text{sym}} = \frac{V_n - V_p}{2\delta} = B_2 \rho + B_8 \rho^{\alpha+1} + \frac{1}{2} B_4 c_k \rho^{5/3} + \mathcal{O}(\delta^2). \quad (15)$$

The symmetry energy coefficient of nuclear matter J is written as [20]

$$J = \frac{1}{2} B_2 \rho + \frac{1}{2} B_8 \rho^{\alpha+1} - \frac{1}{24} \Theta_s c_k \rho^{5/3} + \frac{1}{3} \left(\frac{\hbar^2}{2M} \right) c_k \rho^{2/3} \quad (16)$$

with $\Theta_s = 3t_1 x_1 - t_2 (4 + 5x_2)$. The Θ_s term and the last term of Eq. (16) give the contributions of the effective mass [7] and the kinetic energy to the J , respectively. From the above equations for V_{sym} and J , one can obtain the following relation between them:

$$J = \frac{1}{2} V_{\text{sym}} - \frac{1}{24} [\Theta_s + 6B_4] c_k \rho^{5/3} + \frac{1}{3} \left(\frac{\hbar^2}{2M} \right) c_k \rho^{2/3}. \quad (17)$$

A similar equation is previously proposed in Ref. [21] based on perturbation theory,

$$J = \frac{1}{2} V_{\text{sym}}(k_F) + \frac{1}{6} k_F \left[\frac{\partial V_0(k_m)}{\partial k_m} \right]_{k_m=k_F} + \frac{1}{3} \left(\frac{\hbar^2}{2M} \right) k_F^2. \quad (18)$$

Due to the uncertainty of choosing the interaction parameters, there exists a large uncertainty for the value of V_{sym} in different models. In Fig. 3(a), we show the calculated symmetry potential V_{sym} of nuclear matter with 78 Skyrme forces. The V_{sym} has a value of about 10 ~ 50 MeV according to the calculations. Brueckner-Hartree-Fock calculations show that the value of V_{sym} is about 25 MeV [22]. These calculations indicate that the value of V_{sym} is comparable to that of the symmetry energy coefficient J , which is about 30 MeV.

For finite nucleus, the isospin-asymmetric part V_s of the single-particle potential should slightly differ from the value of V_{sym} . With the density distributions of nuclei obtained in Ref. [8], we calculate the potential depth of protons and neutrons for a large number of nuclei. We find that the difference $V_n - V_p$ increases linearly with the isospin asymmetry I [see Fig. 3(b)]. The average value for the isospin-asymmetric part V_s can be obtained by linearly fitting the calculated results. The obtained values of V_s are 17.0 and 26.9 MeV with SLy4 [23] and SkM* [15] forces, respectively. In Ref. [24], the authors found that the experimental Fermi energies of a number of magic nuclei can be well described with a value of 23.2 MeV for V_s . The a_{sym} in this work has a value of about 23 ~ 24 MeV for heavy nuclei which is roughly comparable to the obtained values of V_s . In the first round of searching for the optimal parameters of the proposed mass formula, we treat V_s as a free parameter and find that the obtained value of V_s is very close to that of a_{sym} . So we empirically set and assume $V_s \approx a_{\text{sym}}$ in the improved mass formula for simplification.

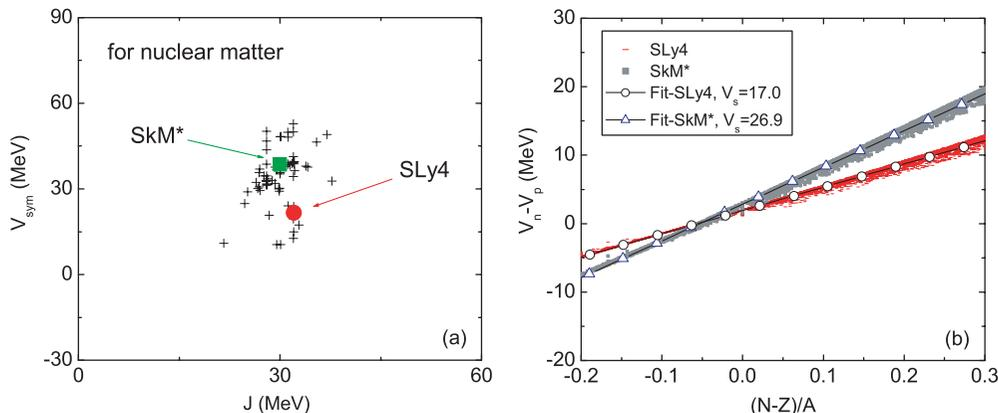


FIG. 3. (Color online) (a) Symmetry potential V_{sym} of nuclear matter with 78 Skyrme forces. (b) The difference between the potential depth of neutrons and of protons as a function of mass asymmetry. The circled curve and the triangled curve denote the results fitted to the calculated results with SLy4 (short red dashes) and SkM* force (small gray squares) for a large number of nuclei, respectively.

E. Model parameters

From the above discussions, one can see that the macroscopic and microscopic parts in the proposed mass formula are closely connected to each other through the coefficient a_{sym} of the symmetry energy and other isospin-dependent model parameters. The number of model parameters is considerably reduced compared with the finite-range droplet model (FRDM) in which the number of parameters is about 31 [1]. Here, we have 13 independent parameters, a_v , a_s , a_c , c_{sym} , κ , a_{pair} , g_1 , g_2 , c_1 , V_0 , r_0 , a , λ_0 , for the nuclear mass. By varying these parameters and searching for the minimal deviation of the 2149 nuclear masses from the experimental data, we obtain a parameter set labeled as WS, which is listed in Table I. To find the minimal energy $E(A, Z, \beta)$ with respect to a set of deformation parameters for a given nucleus, the downhill searching method is adopted. We re-execute the downhill algorithm for several times starting from different initial deformation parameters in order to find the lowest energy of a nucleus from some possible local minima on the energy surface $E(A, Z, \beta)$. In the calculation of nuclear masses with the obtained binding energies, the electron binding energies are not

TABLE I. Model parameters of the mass formula.

Parameter	WS
a_v (MeV)	-15.5841
a_s (MeV)	18.2359
a_c (MeV)	0.7173
c_{sym} (MeV)	29.2876
κ	1.4492
a_{pair} (MeV)	-5.5108
g_1	0.00862
g_2	-0.4730
c_1	0.7274
V_0 (MeV)	-47.4784
r_0 (fm)	1.3840
a (fm)	0.7842
λ_0	26.3163

included. In the parameter searching procedure, the downhill searching method and the simulated annealing algorithm [25] are incorporated. The former is used for the parameters of the microscopic part, while the latter is for the macroscopic part.

III. RESULTS AND DISCUSSION

In this section, we first show the calculated rms deviations of the nuclear masses and of the neutron separation energies. In addition, the change of magic number in light neutron-rich nuclei and the shape coexistence phenomena for some nuclei have been checked with the model. Then, the shell corrections of superheavy nuclei and the location of the center area of the superheavy island are investigated with the proposed mass formula.

A. Test of the model

The corresponding rms deviations of nuclear masses for the 2149 measured nuclei with the parameter set WS is listed in Table II. In addition, the results of FRDM and Hartree-Fock Bogoliubov (HFB-14 [3] and HFB-17 [4]) are also listed for comparison. N_p denotes the corresponding number of parameters used in each model. Compared with the FRDM, the rms error for the 2149 nuclear masses is considerably reduced with WS, from 0.656 to 0.516 MeV. The number of parameters in the model is reduced from 31 to 15 (including the two parameters γ and p used in the Strutinsky procedure). One should note that several (about 12) of the

TABLE II. rms σ deviations between the data from AME2003 [6] and predictions of several models (in MeV). The line $\sigma(M)$ refers to all the 2149 measured masses and the line $\sigma(S_n)$ to the 1988 measured neutron separation energies S_n . The calculated masses with FRDM are taken from Ref. [2]. The masses with HFB-14 and HFB-17 are taken from Refs. [3] and [4], respectively.

	FRDM	HFB-14	HFB-17	WS
$\sigma(M)$	0.656	0.729	0.581	0.516
$\sigma(S_n)$	0.399	0.598	0.506	0.346
N_p	31	24	24	15

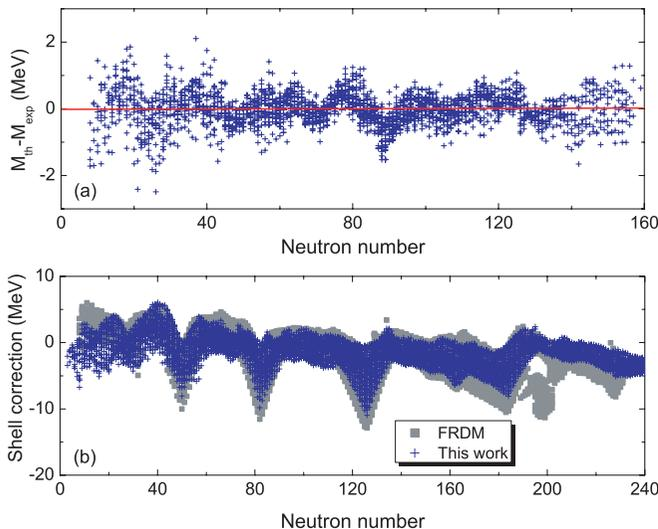


FIG. 4. (Color online) (a) Deviations between the calculated nuclear masses from the experimental data. (b) Calculated shell corrections ΔE of nuclei (crosses). The squares denote the microscopic energy of nuclei with the FRDM model (column E_{mic} of the table in Ref. [2]).

FRDM parameters were prefixed by considerations other than masslike data before making the fit [1,2] and also that the fit in the FRDM included data on fission barriers in addition to masses. In this work, only the precisely measured nuclear masses are involved in the fit. Compared with the standard Hartree-Fock Bogoliubov (HFB) approach, the CPU time used in the calculation of nuclear mass table is much shorter with the proposed mass formula. The obtained rms error for the 1988 measured neutron separation energies S_n with our model is obviously smaller than those of HFB calculations [3,4].

Figure 4(a) shows the deviations between the calculated nuclear masses in this work from the experimental data. In Fig. 4(b), we show the calculated shell corrections ΔE of nuclei with our model and the microscopic energy (mainly including the shell correction and the deformation energy) obtained in the finite-range droplet model. For intermediate and known heavy nuclei, the results of the two approaches are comparable and both of them reproduce the known magic numbers very well. The deviations are large for light nuclei and superheavy nuclei. Our calculations show that the shell corrections of nuclei with about $N = 16$ are much larger (in absolute value) than those from the FRDM. As an example, the shell correction of ^{24}O is calculated and has a value of -4.6 MeV with WS. Experimentally, it is thought that ^{24}O is a doubly magic nucleus from the observed decay energy spectrum and the high-lying first excited 2^+ state (above 4.7 MeV) [26], which is consistent with our calculations. The obtained shell corrections with WS for ^{20}C , ^{22}C [27], and ^{23}N are -4.2 , -5.1 , and -4.3 MeV , respectively. Some theoretical and empirical studies [26,28] have shown that in the neutron-rich nuclei the magic numbers such as $N = 14$ or 16 can arise, which is in agreement with our calculations. It is known that the shell correction strongly depends on the single-particle potential adopted. The isotopic dependence of the spin-orbit strength and the symmetry potential adopted

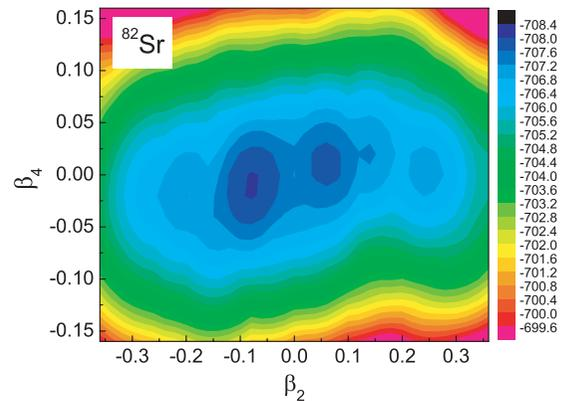


FIG. 5. (Color online) Potential energy surface $E(\beta_2, \beta_4)$ of ^{82}Sr .

in this work differs from that in the FRDM, which leads to the different shell correction from the two models. Our results for the neutron-rich nuclei with about $N = 16$ look more reasonable qualitatively.

To further test the model, we study the potential energy surface $E(\beta_2, \beta_4)$ of some nuclei. In Ref. [29], the authors observed the shape coexistence phenomena for nuclei ^{82}Sr and Kr isotopes from the low- and high-spin states. The shape coexistence phenomena of these nuclei could be observed from the corresponding potential energy surface. In Fig. 5, we show the calculated potential energy surface of ^{82}Sr . The coexistence of oblate and prolate deformed configurations can be clearly observed. The similar coexistence phenomena for Kr isotopes can also be observed with our model.

B. Shell corrections of superheavy nuclei

The precise calculation for the shell corrections of superheavy nuclei is of great importance for the synthesis of new superheavy nuclei, especially for the prediction of the location of the superheavy island. Furthermore, the fission barriers of superheavy nuclei are roughly estimated by the values of the corresponding shell corrections [18,30] since in general the macroscopic fission barriers disappear at the superheavy region. It is known that the fission barrier is a very sensitive parameter in the realistic calculations for the survival probabilities of the produced compound nuclei. It is therefore necessary to investigate the shell corrections of superheavy nuclei.

In Table III, we list the calculated shell corrections ΔE of some nuclei. The corresponding microscopic energy obtained in the FRDM are also listed for comparison. For superheavy nuclei such as nucleus $^{292}114$, the microscopic energies obtained with the FRDM are much lower (absolute value larger about $2 \sim 3\text{ MeV}$) than our calculated ΔE . Because these nuclei are (nearly) spherical in shape according to the calculations. It follows that the deviations of shell energies between the two models are about $2 \sim 3\text{ MeV}$ for nuclei around $^{292}114$. Because the shell correction cannot be measured directly, it is still difficult to quantitatively compare the reliability of model through the calculated shell corrections of nuclei. In addition, we study the central area of the superheavy island based on the calculated shell energies. Figure 6 shows the contour plot of

TABLE III. Shell corrections of some nuclei (in MeV). The data of FRDM are taken from the microscopic energies E_{mic} of the table in Ref. [2].

	^{16}O	^{24}O	^{40}Ca	^{48}Ca	^{90}Zr	^{132}Sn	^{208}Pb	^{270}Hs	$^{288}114$	$^{292}114$	$^{298}114$	$^{294}116$
WS	-0.7	-4.6	2.0	-1.2	-1.3	-9.8	-11.0	-6.4	-5.3	-6.1	-6.1	-6.2
FRDM	2.1	0.3	2.3	0.1	-1.6	-11.6	-12.8	-6.5	-7.8	-8.9	-7.6	-8.7

the calculated shell-correction energies of heavy nuclei. The black squares in Fig. 6(a) denote the nuclei with microscopic energies of $-(6 \sim 7)$ MeV in the FRDM calculations. One can see that both models give similar magic numbers for heavy nuclei. Figure 6(b) shows the shell corrections of nuclei in the superheavy region. The crosses denote the calculated nearly spherical nuclei ($|\beta_2| \leq 0.01$) with WS. The predicted superheavy island according to the obtained shell corrections of nuclei looks flat. Along nuclei with $Z = 114$ or $N = 178$, one can see a slightly deeper valley in the contour plot of shell corrections. The calculated deformations of nuclei demonstrate that the nuclei with $N = 184$ are (nearly) spherical in shape. However, the maximum shell correction occurs at $N = 178$ instead of $N = 184$, which is consistent with the results in Refs. [30,33]. The analysis about the shift of the shell correction from $N = 184$ to $N = 178$ is given in Ref. [30]. According to the calculations, the superheavy nuclei $^{288,289}114$ produced in the “hot” fusion reaction $^{48}\text{Ca} + ^{244}\text{Pu}$ [31] (the corresponding compound nucleus is $^{292}114$) are close to this central area of the island. The half-lives of these nuclei are in the order of seconds [31], which is much shorter than those of known stable nuclei. The measured short half-lives of nuclei in superheavy region seem to indicate that the shell corrections of these nuclei are probably not very large.

Figure 7 shows the deviations of the calculated nuclear masses with the proposed model from the results of FRDM and HFB-17. The shades denote the region with deviations smaller than 2 MeV. The results for highly neutron-rich heavy nuclei from the three models have large deviations. The results of our model are relatively close to those of HFB-17 for most nuclei.

IV. SUMMARY

In this article we proposed a semiempirical nuclear mass formula based on the macroscopic-microscopic approach. The isospin effects in both macroscopic and microscopic part of the formula are self-consistently considered, with which the number of model parameters is considerably reduced compared with the finite-range droplet model and the rms deviation of the calculated masses from the 2149 measured nuclear masses is reduced by 21% and falls to 0.516 MeV. The CPU time used in the calculation of the nuclear masses for the whole nuclear chart is much shorter than that with the microscopic mass formula models. At the same time, the consistency of the model parameters between the macroscopic and microscopic parts greatly promotes the credibility of extrapolations in the macroscopic-microscopic approach.

In order to extend the mass formula to superheavy nuclei and the nuclei far from the β -stability line, we pay a special attention to study the isospin and mass dependence of the model parameters, including the symmetry energy coefficient and the symmetry potential. Those studies are based on the Skyrme energy-density functional approach together with the extended Thomas-Fermi approximation. Since more sufficiently considering the isospin effects of the model parameters, the formula could systematically study superheavy nuclei and the nuclei far from the β -stability line.

To further test the model, the appearance of new magic number $N = 16$ in light neutron-rich nuclei and the shape coexistence phenomena for some nuclei have been examined with the model. Our results are in good agreement with some experimental and theoretical studies. The predicted

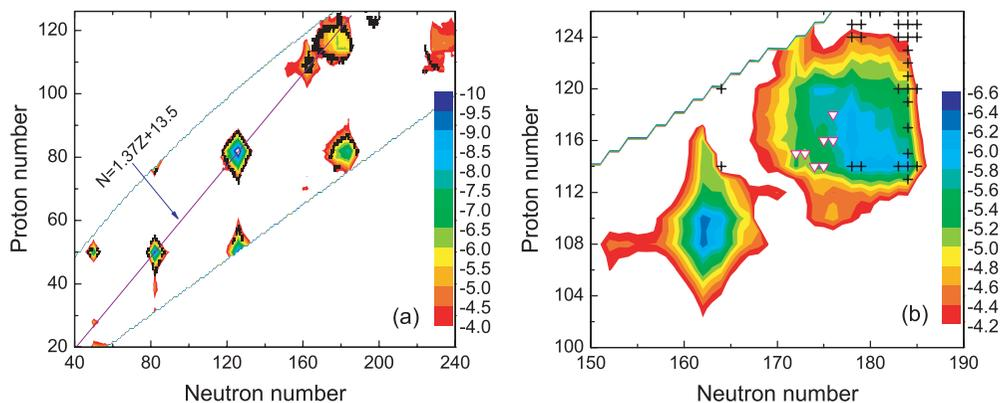


FIG. 6. (Color online) (a) Shell-correction energies ΔE of nuclei. The black squares denote the nuclei with microscopic energies of $-(6 \sim 7)$ MeV in the FRDM calculations. The straight line passes through the areas with the known heavy magic nuclei. (b) Shell-correction energies of nuclei in the superheavy region. The crosses denote the nearly spherical nuclei (calculated $|\beta_2| \leq 0.01$) and the triangles denote the synthesized superheavy nuclei in the “hot” fusion reactions [31,32].

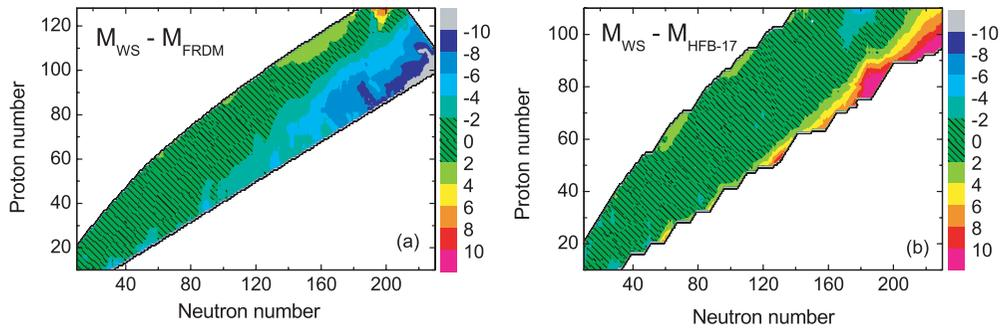


FIG. 7. (Color online) Deviations of the calculated nuclear masses in this work from the results of FRDM (a) and HFB-17 (b), respectively. The calculated masses with FRDM and HFB-17 are taken from Refs. [2] and [4], respectively. The shades denote the region with deviations smaller than 2 MeV.

superheavy island according to the obtained shell corrections of nuclei looks flat. Along nuclei with $Z = 114$ or $N = 178$, we find a relatively deeper valley in the contour plot of shell corrections. The shell corrections of nuclei around $^{292}114$ are about -6 MeV and much smaller (in absolute value) than the corresponding results from the finite-range droplet model. The calculated nuclear masses for highly neutron-rich heavy nuclei from the three different models have large deviations. The results of our model are relatively close to those of HFB-17 for most nuclei.

ACKNOWLEDGMENTS

We thank Professor W. Scheid for a careful reading of the manuscript. We also thank Professor Zhuxia Li and an anonymous referee for valuable suggestions. This work was supported by the National Natural Science Foundation of China, Nos. 10875031, 10847004, and 10865002. The obtained mass tables with the proposed formula are available from <http://www.imqmd.com/wangning/publication.html>.

-
- [1] D. Lunney, J. M. Pearson, and C. Thibault, *Rev. Mod. Phys.* **75**, 1021 (2003).
 - [2] P. Möller, J. R. Nix *et al.*, *At. Data Nucl. Data Tables* **59**, 185 (1995).
 - [3] S. Goriely, M. Samyn, and J. M. Pearson, *Phys. Rev. C* **75**, 064312 (2007).
 - [4] S. Goriely, N. Chamel, and J. M. Pearson, *Phys. Rev. Lett.* **102**, 152503 (2009).
 - [5] J. Duflo and A. P. Zuker, *Phys. Rev. C* **52**, R23 (1995).
 - [6] G. Audi, A. H. Wapstra, and C. Thibault, *Nucl. Phys. A* **729**, 337 (2003).
 - [7] J. Bartel and K. Bencheikh, *Eur. Phys. J. A* **14**, 179 (2002).
 - [8] Min Liu, Ning Wang *et al.* *Nucl. Phys. A* **768**, 80 (2006).
 - [9] S. Cohen, F. Plasil, and W. Swiatecki, *Ann. Phys.* **82**, 557 (1974).
 - [10] H. A. Bethe and R. F. Bacher, *Rev. Mod. Phys.* **8**, 82 (1936).
 - [11] J. Mendoza-Temis, J. G. Hirsch, and A. P. Zuker, [arXiv:0912.0882v1](https://arxiv.org/abs/0912.0882v1).
 - [12] J. M. Pearson, *Hyperfine Interact.* **132**, 59 (2001).
 - [13] Michael W. Kirson, *Nucl. Phys. A* **798**, 29 (2008).
 - [14] S. K. Samaddar, J. N. De, X. Vinas, and M. Centelles, *Phys. Rev. C* **76**, 041602 (2007).
 - [15] J. Bartel, Ph. Quentin *et al.*, *Nucl. Phys. A* **386**, 79 (1982).
 - [16] V. M. Strutinsky and F. A. Ivanjuk, *Nucl. Phys. A* **255**, 405 (1975).
 - [17] R. N. Sagaidak and A. N. Andreyev, *Phys. Rev. C* **79**, 054613 (2009).
 - [18] C. Shen, Y. Abe *et al.*, *Int. J. Mod. Phys. E* **17**, 66 (2008).
 - [19] S. Cwoik, J. Dudek *et al.*, *Comput. Phys. Commun.* **46**, 379 (1987).
 - [20] E. Chabanat, P. Bonche *et al.*, *Nucl. Phys. A* **627**, 710 (1997).
 - [21] K. M. Khanna, D. Jairath, and P. K. Barhai, *Czech. J. Phys. B* **27**, 498 (1977).
 - [22] W. Zuo, L. G. Cao, B. A. Li, U. Lombardo, and C. W. Shen, *Phys. Rev. C* **72**, 014005 (2005).
 - [23] E. Chabanat, P. Bonche *et al.*, *Nucl. Phys. A* **635**, 231 (1998).
 - [24] J. P. Jeukenne, C. Mahaux, and R. Sartor, *Phys. Rev. C* **43**, 2211 (1991).
 - [25] A. Corana, M. Marchesi *et al.*, *ACM T. Math. Software* **13**, 262 (1987).
 - [26] C. R. Hoffman, T. Baumann, D. Bazin *et al.*, *Phys. Lett. B* **672**, 17 (2009).
 - [27] K. Tanaka, T. Yamaguchi *et al.*, *Phys. Rev. Lett.* **104**, 062701 (2010).
 - [28] Raj K. Gupta *et al.*, *J. Phys. G: Nucl. Part. Phys.* **32**, 565 (2006), and references therein.
 - [29] A. Petrovici *et al.*, *Prog. Part. Nucl. Phys.* **43**, 485 (1999).
 - [30] P. Möller, G. A. Leander, and J. R. Nix, *Z. Phys. A* **323**, 41 (1986).
 - [31] Yu. Ts. Oganessian, V. K. Utyonkov *et al.*, *Phys. Rev. C* **69**, 054607 (2004).
 - [32] Yu. Ts. Oganessian, V. K. Utyonkov *et al.*, *Phys. Rev. C* **74**, 044602 (2006).
 - [33] E. O. Fiset and J. R. Nix, *Nucl. Phys. A* **193**, 647 (1972).